Proceedings of the Institution of Mechanical Engineers, Part L: Journal of Materials: Design and Applications,
Available online 31 October 2025, Article number 14644207251382566. DOI:10.1177/14644207251382566

PLAIN WEAVE GLASS-FIBRE COMPOSITE JOINTS WITH CO_2 LASER ABLATION ARCHITECTED TREATMENTS

Luiza Soares, Thayane Ferreira, Alberto Campuzano, Marzio Grasso, Pedro Camanho, Fabrizio Scarpa, Tulio Panzera

Abstract: Glass Fibre Reinforced Polymers (GFRP) are particularly notable for their cost-effectiveness and versatility, finding widespread applications across aerospace, automotive, marine, medical, and sport industries. While the use of adhesive joints in GFRPs is widespread, laser ablation as a surface treatment prior to joining remains relatively unexplored. This study investigates the effects of laser ablation parameters, specifically scanning speed and power, on the surface characteristics of plain weave GFRP. Single-lap shear tests compare untreated and laser-treated joints with different architected groove spacings. Higher scanning speeds, particularly with 0.5 mm spacing, reduce fibre damage, whereas higher laser power levels increase it. Laser treatment improves shear strength by 19%, due to improved mechanical interlocking between the adhesive and the treated surface. When fibres exposure is carefully controlled, the strength of the joints improves by up to 60%. However, excessive resin degradation lowers performance; this indicates that balancing surface roughness and preserving surface integrity is critical to optimise laser ablation treatments.

Keywords: Bonded joints; Glass Fibre Reinforced Polymer; Laser ablation; Single Lap Testing, Surface treatment.

1. Introduction

The use of composite materials is affecting significantly engineering sectors such as aerospace, automotive, naval, construction and sports. The integration of composites enables a significant reduction in structural weight, which in turn enhances energy efficiency and overall performance [1,2]. Joints between two or more composite materials are critical in many applications. The use of conventional mechanical fasteners, such as welds, rivets, screws, or nuts, runs counter to the objective of lightweight structures by adding additional mass [3,4]. Moreover, these mechanical fasteners introduce stress concentrators into the structure and can cause defects during the drilling of laminates for joint assembly, including tearing and delamination at both the upper and lower layers [5]. In contrast, adhesive joints have demonstrated excellent resistance to corrosion and fatigue, alongside notable improvements in product performance and durability [5, 6]. However, the design, manufacture, and predictive modelling of composite joints remain critical factors in the advancement of composite structures [3, 6].

The performance of adhesive joints is influenced by three critical factors: service conditions, which involve the mechanical loads and environmental exposures the joints face; composition, including the types of adhesives and the materials being bonded; and the bonding process, encompassing surface preparation and adhesive curing techniques [3].

Reluctance to adopt bonding technologies often arises from uncertainty about the compatibility of structural adhesives with different substrates, which requires careful pre-treatment to ensure effectiveness. Surface treatments fall into three broad categories: mechanical methods like sanding or blasting—though these can compromise fiber integrity—chemical approaches using solvents or etching agents, and physicochemical techniques such as plasma, corona, UV, or ozone treatments. These physicochemical approaches modify surface energy and improve adhesion without requiring physical contact [7, 8].

Laser ablation surface treatment is distinguished by its precision, localised control, and capacity to simultaneously modify both surface topography and chemistry. Its effectiveness as a pre-treatment method is linked to the selective removal of the matrix from the composite surface, thereby exposing the carbon fibres, increasing surface energy and substrate wettability, altering surface morphology to enhance roughness, and promoting mechanical interlocking [9–11].

The removal of the matrix from the surface of the laminate without damaging the fibres is crucial for improving adhesion and the structural integrity of the composite [12, 13]. Conversely, when fibres are damaged due to excessive laser power, a significant reduction in the shear strength of the joints is observed [14, 15]. This suggests that laser ablation allows the adhesive to bond directly to the load-bearing fibres, effectively eliminating the need for drilled holes or mechanical fasteners.

Additionally, this process removes from the surface any release agents that could adversely affect adhesion [16], as well as potential contaminants, thereby facilitating direct bonding without compromising quality [17]. Surface treatment via laser ablation has proven to be an effective method for enhancing the shear strength of adhesive joints. Andarabi et al. [18] evaluated laser surface treatment for aluminium adhesive joints and concluded that the process created micro- and nano-scale topographies on the aluminium substrate. This

Published by SAGE. This is the Author Accepted Manuscript issued with: Creative Commons Attribution License (CC:BY 4.0).
The final published version (version of record) is available online at DOI:10.1177/14644207251382566. Please refer to any applicable publisher terms of use.

increased the interfacial area and promoted mechanical interlocking at the bonded interface. In some cases, laser ablation also led to cohesive failure, further demonstrating the effectiveness of laser surface treatment for improving the performance of adhesively bonded joints. Similarly, Wu et al. [19] investigated the effect of laser ablation surface treatment on the performance of adhesively bonded aluminium joints. They found that higher laser powers significantly improved joint strength and increased the occurrence of cohesive failure. These improvements are attributed to the direct correlation between a higher laser power and increased surface roughness of the treated substrates.

Li et al. [20] demonstrated the importance of carefully evaluating both groove depth and spacing when using laser treatment to pretreat CFRP (Carbon Fibre Reinforced Polymer) surfaces for adhesive bonding. An optimal groove depth is essential, as excessively deep grooves can cause air bubbles to form during curing, which weakens the joint strength. Groove spacing is also a key factor affecting performance; increasing the distance between grooves reduces the contact area and mechanical interlocking, leading to lower shear strength. Among the groove patterns tested, those oriented at 90°, perpendicular to the applied load, provided the greatest improvement in joint performance. Similarly, Zou et al. [21], Luo et al. [22], and Musiari et al. [9] have shown that laser treatment improves surface roughness and energy, thus enhancing mechanical interlocking between materials.

Badami et al. [23] and Wang et al. [24] have also demonstrated that surface roughness and surface free energy are critical factors influencing bonding strength. Naat et al. [25] also emphasised the importance of selecting the appropriate surface texture to improve wettability and bonding performance. These findings suggest that laser ablation surface treatment is a promising technique for enhancing the shear strength of adhesive joints, with potential applications across various industries. However, the optimal performance of adhesive joints depends on the careful selection of treatment parameters, including laser speed and power.

As previously mentioned, in addition to surface treatment, the choice of adhesive is crucial for the performance of bonded joints. Epoxy resins provide strong adhesion over a wide temperature range (−150°C to 200°C). Epoxies are also cost-effective, offer formulation flexibility, and cure without releasing volatiles, making them ideal for a variety of applications [26].

While laser treatment to improve the strength of bonded joints has been widely applied to carbon fibre reinforced polymers (CFRP), recent studies have increasingly focused on bonded joints of glass fibre reinforced polymers (GFRP) [27–29]. This is due to GFRP's advantages in terms of ductility, corrosion resistance, and cost-effectiveness, particularly in structural and construction applications.

This work introduces a surface treatment process using laser ablation specifically aimed at enhancing the mechanical interlocking in adhesive joints of glass fibre/epoxy composites—an approach that remains largely unexplored for GFRPs. The study details the various laser process parameters employed, such as scanning speed and power, to achieve effective removal of the outer matrix while maintaining the integrity of the glass fibre filaments or minimising their damage. Surface characterisation is conducted using optical microscopy techniques, and the effectiveness of the treatment is assessed through single-lap shear tests.

The investigation involves the execution of two complementary experiments. The effect of groove spacing on the shear strength of adhesive joints is first assessed. Based on the optimal spacing determined, a subsequent experiment explores the behaviour of a wide range of scanning speed and power parameters, while ensuring no compromise to the fibre surface. This methodology provides deeper insight into the balance between surface roughening for mechanical interlocking and maintaining fibre integrity. Surface characterisation is conducted using optical microscopy techniques, and the effectiveness of the treatment is assessed through single-lap shear tests.

2. Materials and Method

2.1. Materials

Glass Fibre Reinforced Polymers (GFRPs) are manufactured by infusing four layers of plain weave glass fabric (200 g/m²) supplied by Texiglass Brazil. The matrix comprises an epoxy resin (MR M) and a hardener (MR 951), both obtained from Huntsman (Brazil). The resin and hardener are mixed in a 10:1 ratio. The mechanical properties of the matrix phase are detailed in Table 1. These properties are obtained via tensile and compressive testing, following the ASTM D638 and D695, respectively. Bulk density is measured dividing the sample mass by its volume. A Shimadzu testing machine equipped with a 100 kN load cell is used. The final thickness of the GFRP composite is 0.65 mm, and the same epoxy system used during the infusion process

is employed as the adhesive. The laser ablation surface treatment is performed using a Robotec RTJ-1390 CO_2 laser system (150 W, 10.6 μm wavelength). The laser operates in pulsed mode with a frequency of 20 kHz.

Table 1. Epoxy polymer properties.

Properties		Values
Tensile	Modulus of elasticity	1.29 ± 0.05 GPa
	Yield strength	28.75 ± 0.40 MPa
	Strength at failure	27.30 ± 0.71 MPa
Compressive	Modulus of elasticity	1.75 ± 0.08 GPa
	Yield strength	55.34 ± 1.43 MPa
Bulk density		1.17 ± 0.01 g/cm³

2.1.1. Manufacturing the GFRPs

The composites are manufactured by resin infusion. The process is conducted on a sterilised glass plate, taking into account both the fibre layup and the vacuum bag configuration. Initially, a release wax is applied, followed by a liquid release agent to facilitate easy removal of the laminate and ensure a smooth finish after curing. Four layers of cross-ply glass fabric, each measuring 320 × 360 mm² (127 g), are then stacked, followed by the application of release film, peel ply, and flow media. The infusion system is assembled, incorporating tubes, connectors, and valves that enable uniform resin distribution through the fibre layup via vacuum (Figure 1). Prior to infusion, the vacuum bag is held at a pressure of −500 mmHg for 14 hours to check for any air ingress. Once infusion begins, the vacuum pump (Edwards RV5) continues to operate for one hour after the resin has fully saturated the layup. After this, the pump is switched off, but the system is maintained under vacuum for a further 24 hours to allow curing. The resulting GFRP achieves a fibre volume fraction of 52% and a matrix volume fraction of 48%.

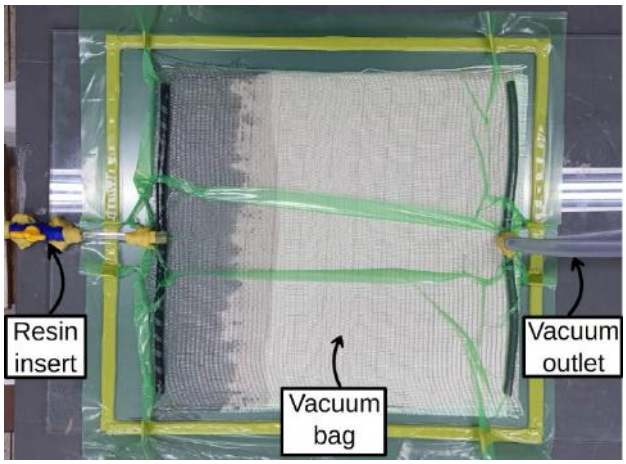


Figure 1. Infusion manufacturing setup.

2.2. Laser ablation setup

Two complementary experiments are conducted to investigate the effects of laser surface treatment on GFRP substrates. The first experiment evaluates the impact of surface architecture—focusing on groove spacing—to determine its effect on the strength of adhesively bonded joints. The grooves are designed to selectively remove the outer polymer matrix surface while preserving the integrity of the fibres. The second experiment examines the effects of matrix removal and potential fibre damage on the mechanical performance of the adhesive joints. Preliminary tests varying laser power, scanning speed, and focal distance were conducted to establish an appropriate range of interest for the final experiments. For the first experiment, the laser focal distance was set to 6 mm, as recommended by the manufacturer. In the second experiment, the focal distance was set to 2 mm to minimize fibre exposure during laser treatment to achieve one of the study conditions (Figure 2). The groove spacing used in the second experiment corresponds to the optimal condition identified in the first.

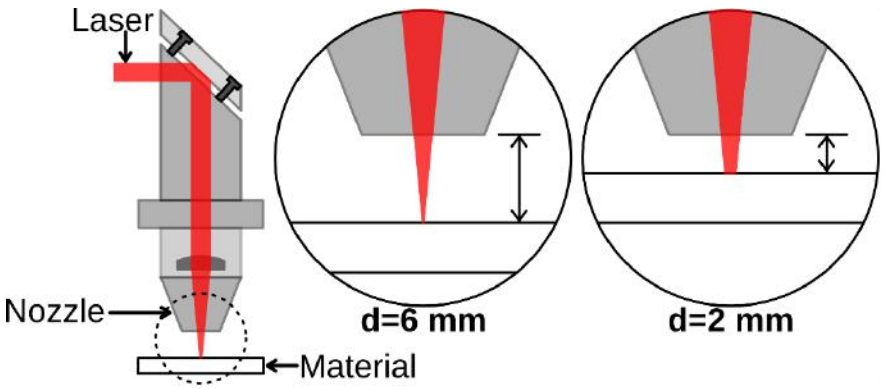


Figure 2. Illustrative diagram of the laser focal distance: Experiment I (d=6 mm) and Experiment II (d=2 mm).

2.2.1. Experiment I

The glass fibre composites are cleaned with alcohol to eliminate the release agent used during infusion. Initially, two laser power settings (15% and 17%, which corresponds 22.5 W to 25.5 W) and two scanning speeds (300 mm/s and 500 mm/s) are considered to evaluate the laser's influence on the grooves, ensuring that the laser removes the outer matrix surface without damaging the fibres. Grooves 100 mm in length are produced using the aforementioned parameter combinations, and subsequently, they are analysed under an optical microscope. An additional setup at 15% power with an increased scanning speed (700 mm/s) is also conducted to verify fibre integrity.

Due to the weave structure of the fabric used in the cross-ply laminate, fibres oriented at 0° (parallel) and 90° (transverse) relative to the laser path are observed during the evaluation. When the fibre direction changes, a region known as the "fibre valley" forms, where a thicker resin layer is present (indicated by red arrows). Conversely, in the "fibre peak" areas, the resin layer above the fibres is thinner (indicated by blue arrows) (Figure 3a).

An optimal combination of laser power and scanning speed (15% and 700 mm/s) is chosen for the surface treatment via laser ablation. For evaluation in single-lap testing (ASTM D5868 [30]), three distinct surface treatment conditions are considered: (i) an untreated surface (no laser ablation), (ii) a surface treated with laser ablation at a line spacing of 0.25 mm, and (iii) a surface treated with laser ablation at a line spacing of 0.5 mm (Figure 3b).

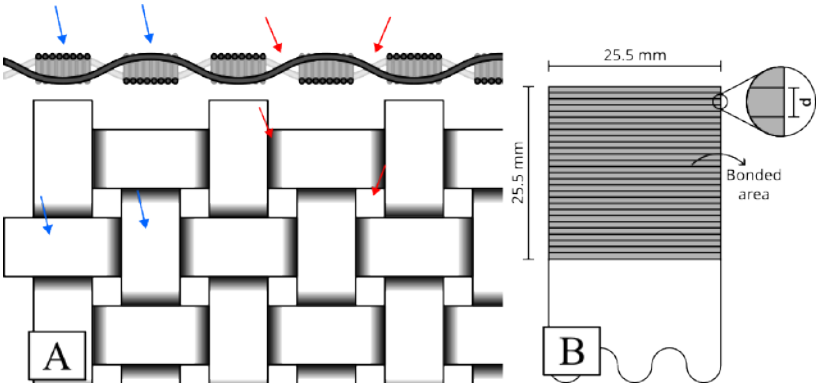


Figure 3. a) Schematic representation of bonded area and b) surface treatment.

2.2.2. Experiment II

Based on the findings of Experiment I, Experiment II is designed to explore the behaviour of a wide range of scanning speed and power parameters without compromising fibre surface, except one used as reference. The grooves produced by laser ablation are 100 mm long. Three speed levels are tested: 500, 700, and 1000 mm/s, with power settings ranging from 11% to 28% of the laser's total output, which corresponds to a range of 16.5 W to 42 W.

An optical microscope (Olympus BX 41P) is employed to analyse the grooves, assess polymer matrix removal, and evaluate fibre integrity. Initially, all combinations of power and speed were tested and evaluated according to four criteria: (i) no polymer removal, (ii) partial polymer removal (when areas of fibre are exposed but without

forming a continuous groove), (iii) complete polymer removal (with the formation of a continuous groove), and (iv) damaged/burnt fibres. Figure 4 presents an example of each of these four possible situations. After this stage, three distinct laser cutting parameters are established to achieve three different surface treatments, as follows: 1) no polymer removal, 2) polymer removal without damaging the fibres, and 3) polymer removal with fibre damage. The laser line spacing used corresponds to the best one identified in Experiment I.

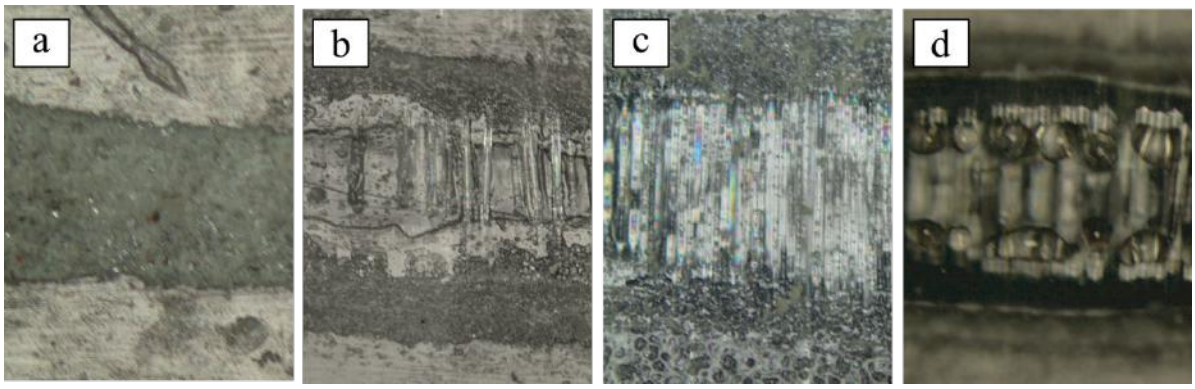


Figure 4. Representative examples of surface conditions: a) no polymer removal, b) partial polymer removal, c) complete polymer removal, and d) fibre damage.

2.2.3. Sigle Lap Shear Testing

The surface treatment involves continuous straight lines orientated transversely to the load direction (Figure 4b). This laser surface treatment is specifically applied to the bonding area, with a spacing of d (mm) between the laser lines (Figure 3b). To ensure precise horizontal and vertical alignment of samples during manufacturing, 3D-printed PLA moulds are designed. These moulds achieve a consistent adhesive thickness of 0.5 mm over a bonding area of 25.4 x 25.4 mm², in accordance with ASTM D5868 [30], as illustrated in Figure 4b. Five samples are fabricated for each condition. The single-lap test is conducted at a speed of 13 mm/min using a Shimadzu AGX-Plus-100 kN testing machine. This test evaluates the maximum load and the corresponding shear stress sustained by the adhesive joints, with stress calculated based on the effective bonding area.

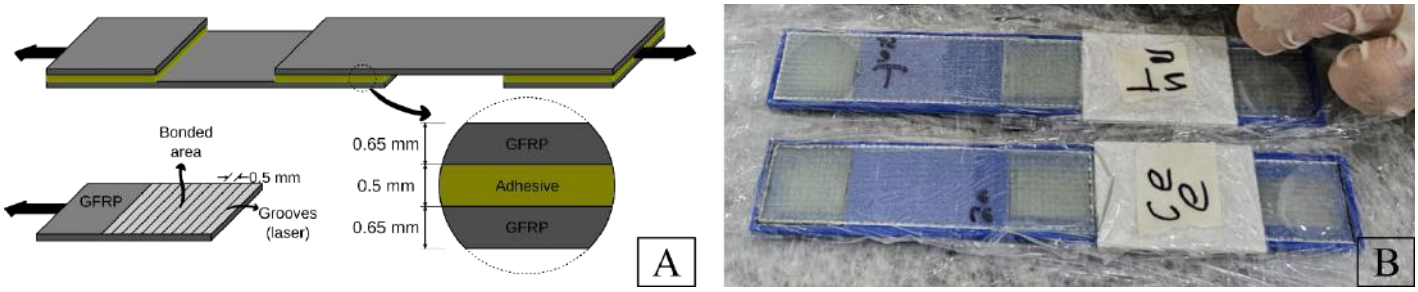


Figure 5. a) Sketch of samples b) fixing of the samples over 3D printed moulds during manufacturing.

When adhesive joints are examined, their failure modes are classified based on the guidelines in the ASTM D5377 [31] standard. Generally, these failures are categorised into three main groups. Firstly, adhesive failure is caused by poor adhesion between the adhesive and the substrate. Secondly, cohesive failure is identified by adhesive remaining on both bonded surfaces, indicating that the adhesive itself has failed rather than its bond to the substrate. Cohesive failures can be further divided into two types: Thin-Layer Cohesive (TLC) and Light Fibre Tear (LFT). Lastly, substrate failure occurs outside the bonded area, which demonstrates that the adhesive joint is stronger than the adherend material [5, 31], as is illustrated in Table 2.

Table 2. Illustration of failure modes

Failure Mode	Representative Image	Description
Adhesive Failure		This is caused by poor adhesion between the adhesive and the substrate, where the adhesive separates cleanly from the substrate surface.

Thin-Layer Cohesive Failure (TLC)		This is characterised by a thin layer of adhesive remaining on one of the surfaces after failure.
Light Fibre Tear (LFT)		This is observed when a thick adhesive layer remains on one side and is minimal or absent on the other, with slight resin and fibre removal at the interface.
Substrate Failure		This occurs outside the bonded area, showing that the adhesive joint is stronger than the adherend material.

3. Results

3.1. Experiment I

3.1.1. Power and Speed Effect

Figure 6 shows microstructure images of the grooves at 10× magnification. At 17% power, both 300 mm/s and 500 mm/s speeds cause severe degradation and melting of the glass fibres in transverse and longitudinal directions. At 15% power and 300 mm/s, similar fibre fusion is observed in both directions. However, at 500 mm/s with 15% power, fibre damage is less pronounced. The fibres remain intact in the transverse direction, and no burning is observed in the longitudinal direction.

Fibre damage is intensified with increasing laser power, whilst it is consistently reduced by increasing scanning speed. Additionally, narrower grooves are produced by higher speeds, as illustrated in Figure 6. An additional setup, conducted at 700 mm/s and 15% power, demonstrates fibres being exposed without any damage in both directions. Based on these findings, Experiment II is focused on the study of a higher range of power and scanning speed on the shear strength of adhesive joints without compromising glass fibres.

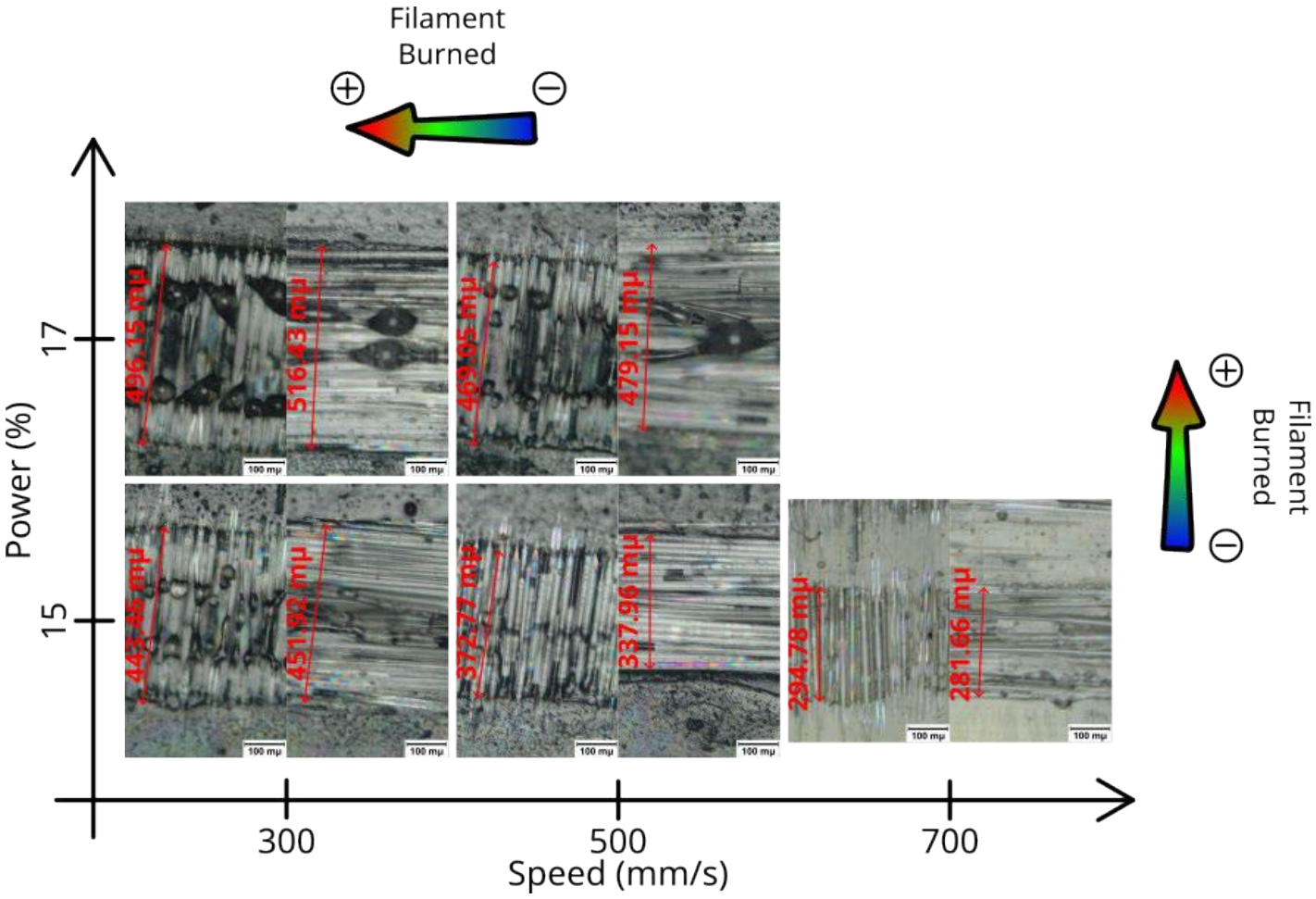


Figure 6. Microstructures after laser treatments at different powers and speeds

3.1.2. Groove Spacing Effect

The surface treatment is set at 15% power and 700 mm/s to verify the groove spacing effect, as this condition effectively removes resin and creates narrow grooves without damaging the glass fibres. As previously mentioned, the weave pattern of the fibre glass fabric causes the laser to run parallel to the fibres in some areas, and perpendicular or transverse to them in others.

Figure 7 shows the treated surface with a line-spacing of 0.5 mm. It is clear that the laser removes the top layer of the matrix phase, revealing the fibres in their peak regions. In the fabric valleys, where the matrix phase is thicker, the fibres remain unexposed. Achieving full removal in these areas necessitates a higher power setting, which causes, in turn, damage to the fibres. In these valley areas, the laser leads to a slight degradation of the polymer, as highlighted by the yellow arrows in the image. It is also noticeable that the laser does not cover the entire surface at 0.5 mm spacing, as indicated in red in the image.

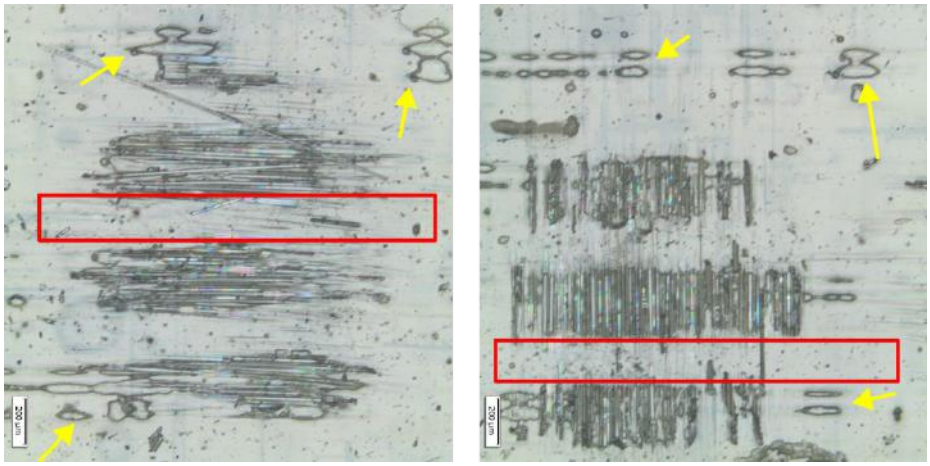


Figure 7. Microstructure after laser treatment with 0.5 mm spacing; longitudinal (left) and transverse (right) fibre directions.

Figure 8 displays the surface treated with a 0.25 mm spacing between the grooves. The grooves overlap, ensuring the entire surface is treated by the laser, which fully exposes the peak regions of the fibres. In the valley regions, greater degradation of the matrix phase is observed compared to the 0.5 mm spacing, as demonstrated by the yellow arrows. This occurs because higher laser energy is caused by overlapping grooves.

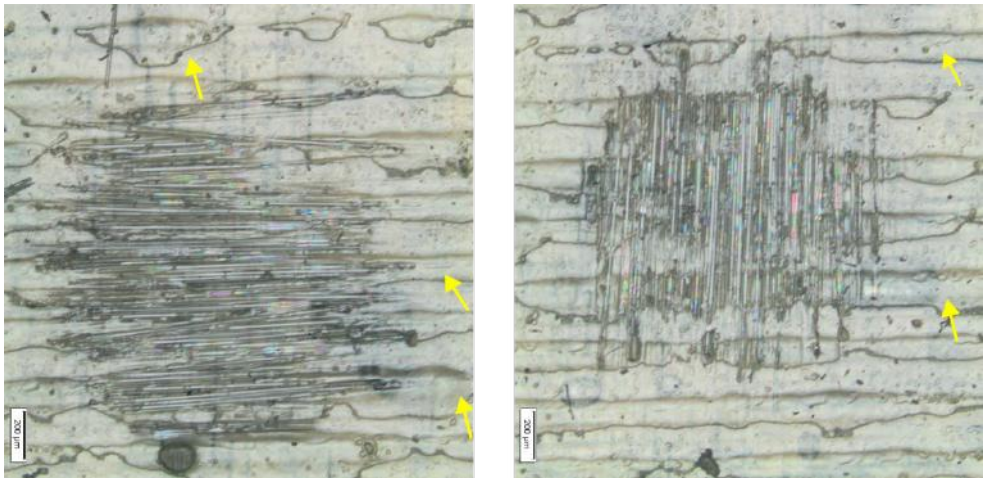


Figure 8. Microstructure after laser treatment with 0.25 mm spacing; longitudinal and transverse fibre directions.

A comparison between three surface conditions, untreated (a), 0.25 mm groove spacing (b), and 0.5 mm groove spacing (c), is illustrated in Figure 9, which displays SEM images of the laser-ablated grooves at a consistent magnification.

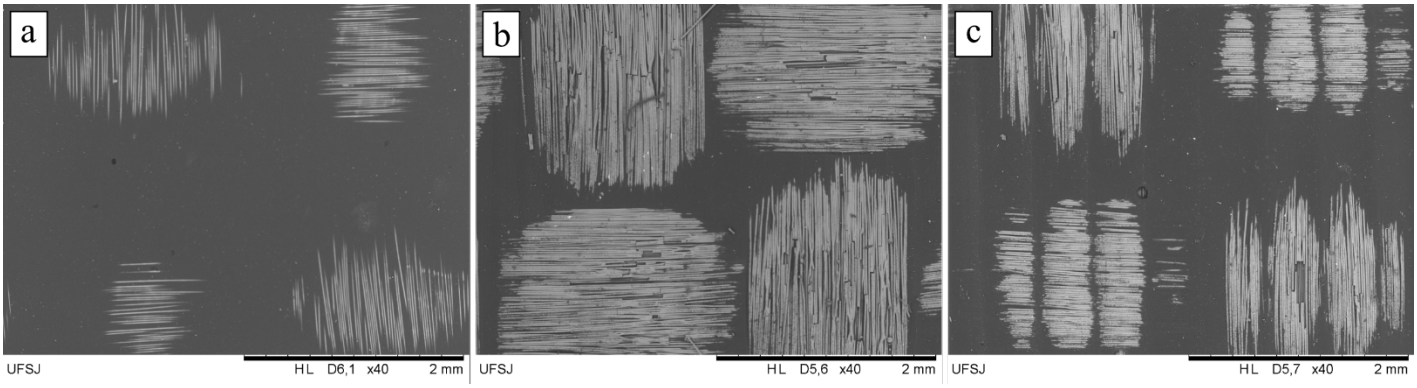


Figure 9. SEM images of surfaces (a) untreated, (b) 0.25 mm and (c) 0.5 mm spaced samples.

3.1.3. Single-lap testing

Table 2 shows the maximum shear force and stress obtained from the single-lap shear testing (Experiment I). Tukey's multiple comparison analysis is conducted at a 95% confidence level, and it reveals statistically different means between all treatments with different letter groups. Figure 10 displays typical force versus displacement curves for each condition. The untreated samples exhibit the lowest shear properties, with values of 3805 N and 5.81 MPa. In contrast, the laser treatment at d = 0.5 mm achieves the highest shear force and stress values, reaching 4621 N and 6.92 MPa. This corresponds to a 19% increase relative to the untreated samples. Comparing the area under the typical curves for each joint type reveals that laser ablation treatments significantly improve energy absorption and fracture resistance.

Table 3. Single lap test results for Experiment I

Surface Treatment	Shear force (N)	Tukey test	Shear stress (MPa)	Tukey test
Untreated	3805 ± 21	C	5.81 ± 0.06	C
d = 0.25 mm	4178 ± 160	B	6.12 ± 2.01	B
d = 0.5 mm	4621 ± 107	A	6.92 ± 0.19	A

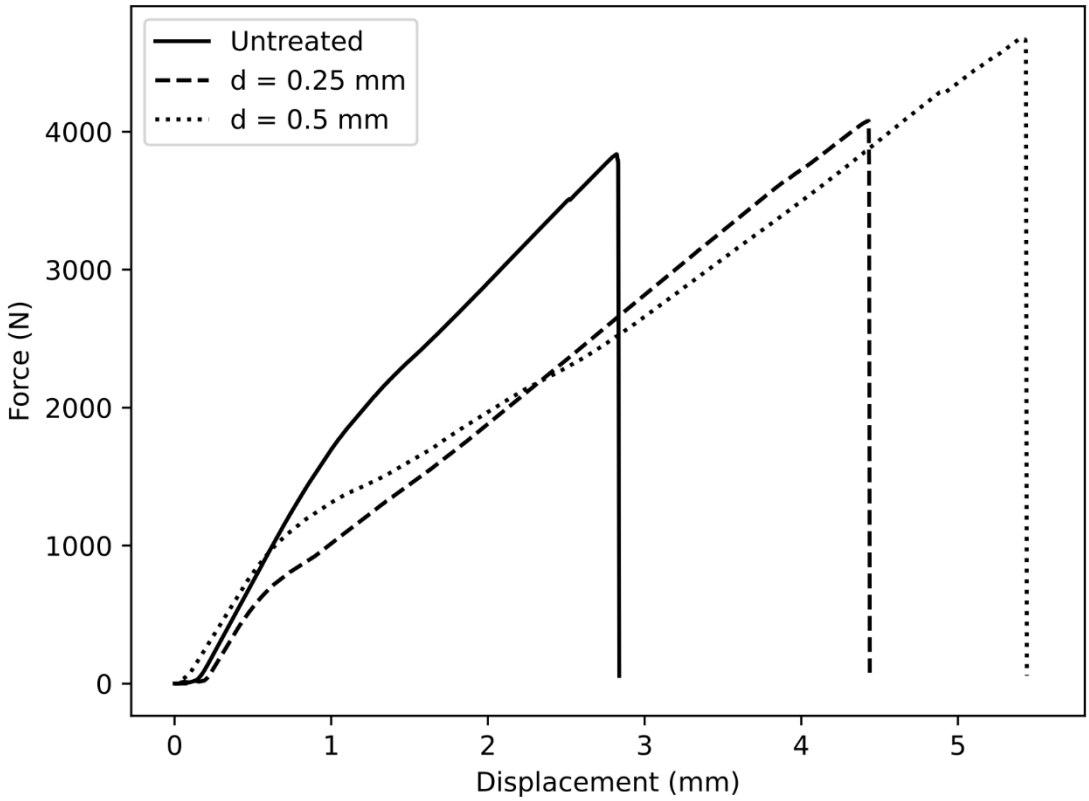


Figure 10. Typical force versus displacement curves obtained via single lap testing.

This study found that a 0.25 mm laser groove spacing, which "scans" the entire surface, leads to more severe polymer degradation (Figure 8) and a reduction in bonded joint strength. Conversely, a 0.5 mm spacing increases mechanical interlocking without excessive resin damage, resulting in stronger bonded joints. As Li et al. [12] reported, mechanical interlocking enhances joint strength while resin degradation diminishes it. Thus, optimizing joint performance requires a balance between these two factors.

The SEM micrographs in Figure 11 illustrate the surfaces of typical samples following a single-lap shear test. The images compare the untreated (a), d = 0.25 mm (b), and d = 0.5 mm (c) surface conditions. In the untreated samples (Figure 11a), regions of adhesive failure are evident (yellow arrows), which indicates a poor bond between the adhesive and the surface. Additionally, some areas exhibit light fibre tear (LFT), where fibres have been exposed. For the treated samples, Figures 11b and 11c show exposed fibres after the removal of the matrix phase and adhesive, a clear sign of enhanced adhesion. Nevertheless, the sample with a d = 0.5 mm spacing still shows small regions of remaining resin (yellow arrows, Figure 11c), pointing to localised adhesive failures. In stark contrast, no adhesive failure is seen for the d = 0.25 mm spacing, as the entire GFRP resin surface was removed, as depicted in Figure 11b. Despite the presence of some adhesive failures, the d = 0.5 mm spacing yields a higher shear strength. This is because the substrate is less damaged, thus requiring a greater force to remove the GFRP resin layer. For the d = 0.25 mm spacing, the force needed to detach the layer is lower, a result of the laser damage to the GFRP resin surface.

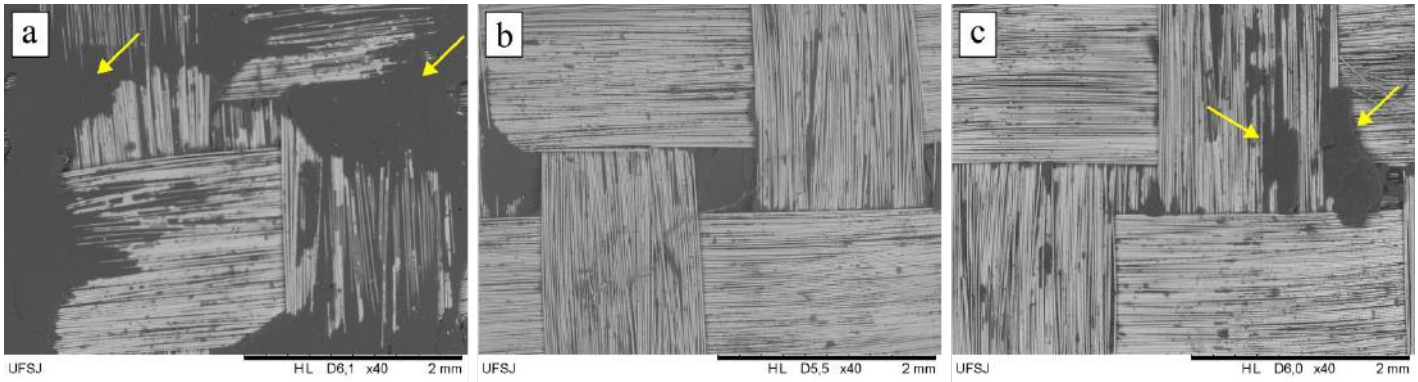


Figure 11.SEM images after failures of (a) untreated, (b) 0.25 mm and (c) 0.5 mm spaced samples.

3.2. Experiment II

3.2.1. Laser parameter effects

Figure 12 illustrates the relationship between polymer removal, laser speed, and power. As power increases, polymer removal increases, whereas higher speeds lead to reduced resin removal. Notably, only power levels at 42 W (28%) cause damage to the fibres. It is observed that power levels below 18 W (12%) don't achieve polymer removal, while powers between 19.5 W (13%) and 22.5 W (15%) result in partial polymer removal. Ablation performed at 19.5 W gives partial removal of the polymer matrix at any speed considered. This means speed affects the partial removal of the matrix at power intensities between 21 W (14%) and 22.5 W (15%). Power levels exceeding 25.5 W (17%) lead to complete polymer matrix removal.

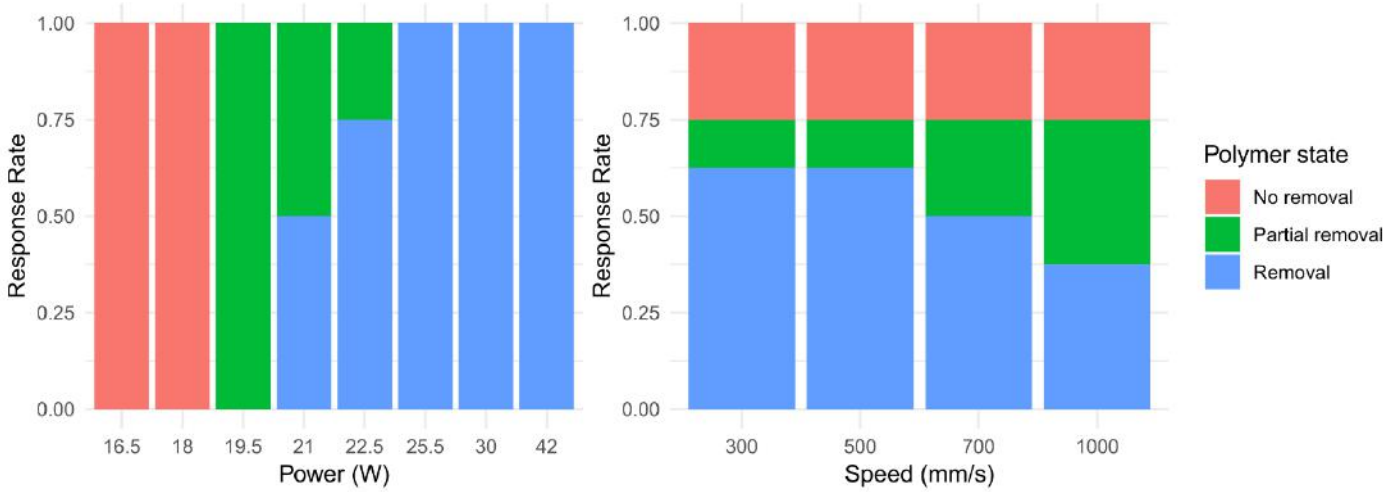


Figure 12. Polymer matrix removal in relation to power and speed levels.

To isolate the impact of power level, a constant laser scanning speed of 700 mm/s is used across three distinct power levels: 18 W, 30 W, and 42 W. Figure 13 displays the resulting GFRP microstructure after laser ablation, with red dashed lines indicating the 700 mm/s laser trajectory.

The 18 W setting is chosen because it doesn't remove the polymer matrix, which allows us to assess the laser's surface influence without forming grooves. The 30 W condition, however, effectively removes the polymer matrix without damaging the fibres, striking an ideal balance between processing effectiveness and material integrity. Finally, the 42 W level demonstrates the effects of high intensity, where both the polymer matrix is removed and fibre damage occurs, resulting in grooves deeper than those created at 30 W. These configurations enable a comprehensive analysis to identify the optimal power level for laser ablation surface treatment in adhesive joints.

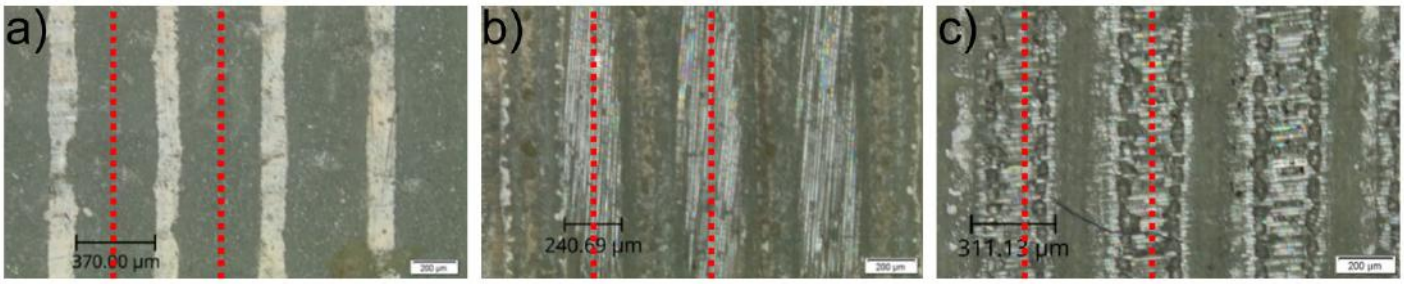


Figure 13. P18 W (a), P30 W(b) and P42 W (c) laser treatments of GFRPs.

3.2.2. Single lap testing

Figure 14 illustrates the typical force-displacement behaviour for each condition, as obtained from single-lap testing. All configurations used a consistent scanning speed of 700 mm/s, but varied in power levels (18 W,

30 W, and 42 W). P18W samples typically fail at approximately 2500 N. In contrast, the mechanical interlocking provided by laser-ablated grooves enables the joints to withstand over 4000 N. A significant enhancement in joint toughness is clearly evident when comparing the area under these force-displacement curves.

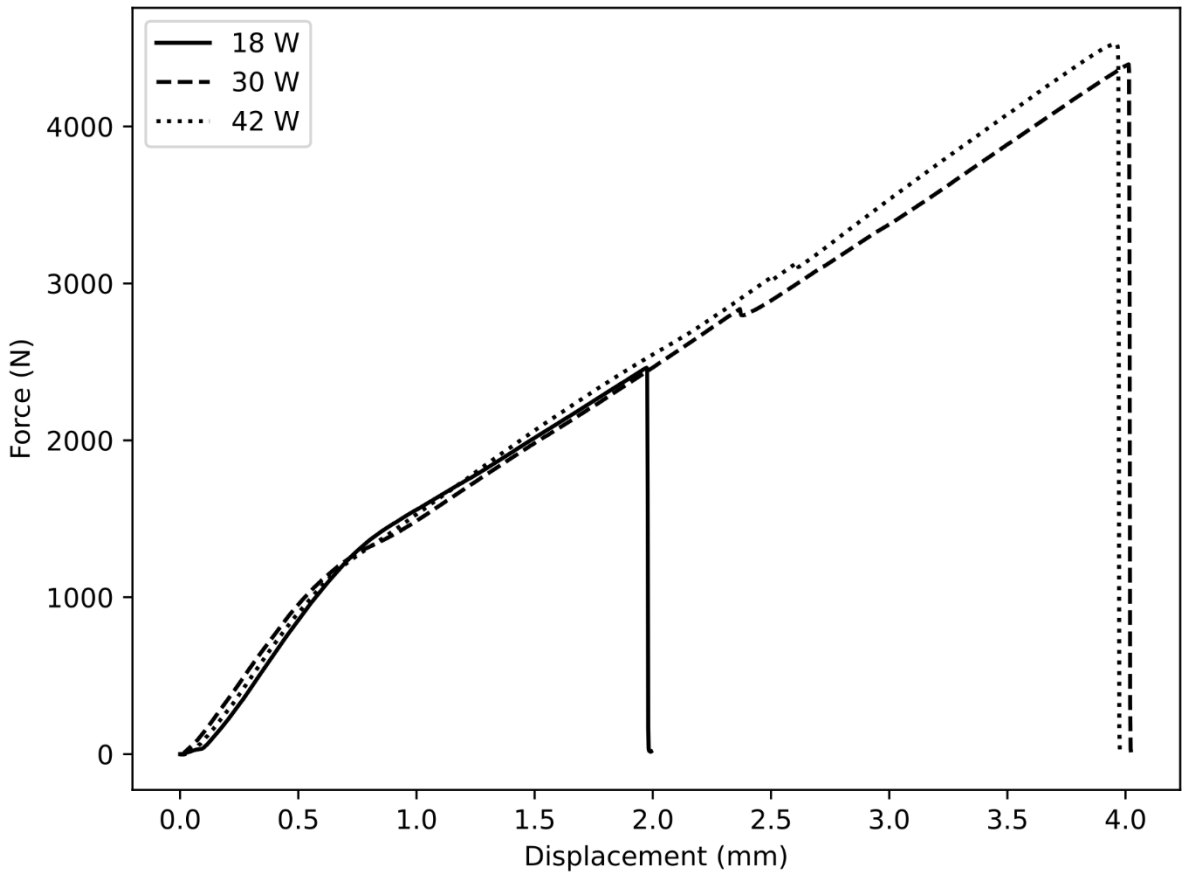


Figure 14. Typical force versus displacement curves obtained via single lap testing.

The surface treatment achieved with the P18W level yields results comparable to those reported by Rangaswamy et al. [32], who used acetone and sandpaper to boost surface roughness. Both treatments exhibit a maximum shear load of approximately 2500 N, demonstrating that laser treatment, even without creating grooves, remains a viable alternative to traditional methods. Analysis of Variance (ANOVA) and Tukey tests are performed at a 95% confidence level, where similar letter groups signify equivalent means. Samples treated with P30W and P42W belong to Letter Group A, indicating that their means are statistically equivalent. Notably, P30W and P42W achieve approximately 60% higher adhesive properties than P18W. Although it is expected that 42 W results in lower joint strength compared to 30 W (as higher power leads to greater material degradation and, consequently, a reduction in joint strength [12]), it is also true that higher power produces deeper grooves and greater surface roughness, which can enhance the strength of bonded joints [19]. This can be seen in Table 3.

Table 4. Single lap testing and Tukey test analysis

Surface Treatment	Shear force (N)	Tukey test	Shear stress (MPa)	Tukey test
P 18 W	2422 ± 248	B	3.82 ± 0.28	B
P 30 W	4070 ± 369	A	5.99 ± 0.66	A
P 42 W	4160 ± 357	A	6.04 ± 0.57	A

Figure 15 shows SEM micrographs of sample surfaces after a single-lap shear test. In the P18W samples (Figure 15a), you can see adhesive failure, where the bond between the adhesive and the substrate has been completely lost. In contrast, the P30W and P42W samples show light fibre tear failure. Exposed fibres are visible in some areas of the P30W sample (Figure 15b) and are fully exposed in the P42W sample (Figure 15c). This failure is more pronounced in the P42W sample, likely due to greater resin degradation and fibre damage, as evidenced by the broken fibres in Figure 15c. Furthermore, Figure 15d, which shows the opposite surface of the P42W sample, reveals fibre fragments that were pulled out along with the GFRP's superficial resin layer. This phenomenon wasn't seen in the other samples.

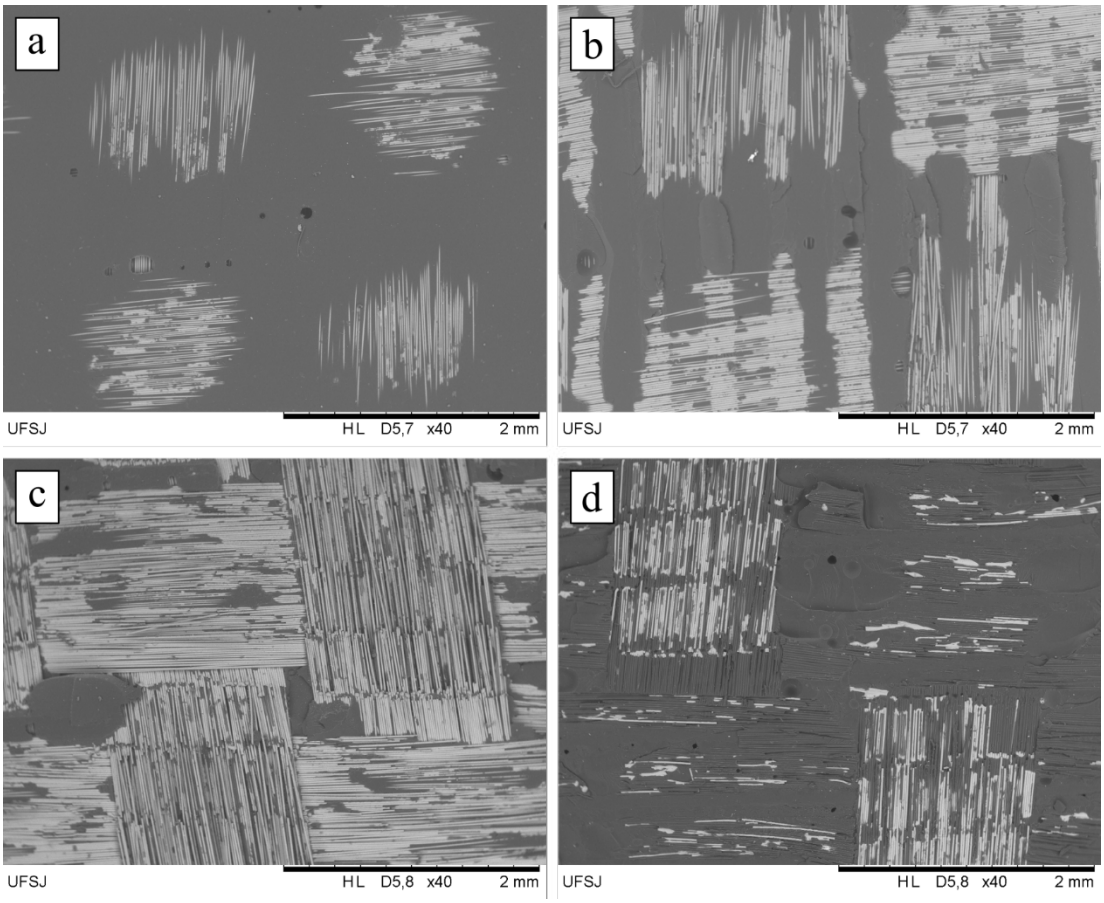


Figure 15. SEM micrographs after failure for treatments with (a) P18W, (b) P30W, and (c–d) P42W.

4. Conclusions

This study assessed plain weave glass fibre composite joints, with a focus on surface treatments performed using laser ablation. Variations in laser power and speed provide an inverse effect on the surface treatment. Increasing laser speed reduces damage to the fibres, while increasing laser power increases it. When comparing laser line spacing (d), composite joints treated by laser ablation showed a 19% increase in shear strength compared to untreated joints. Furthermore, the adhesive failure typically seen in untreated joints was significantly reduced. Among the treated configurations, the 0.5 mm spacing delivered the best performance, as it improved mechanical interlocking without excessively degrading the resin on the GFRP surface. A 60%

increase in the shear strength of adhesive joints is observed to result from polymer surface removal after laser ablation, which leads to groove formation. These grooves act as mechanical interlocks between the adhesive and the bonding surface. While the grooves formed by laser treatment enhance mechanical interlocking and thus increase the shear strength of adhesive joints, the laser process also degrades the matrix phase surface of the GFRP. This degradation can reduce the overall shear strength of the joint. Therefore, optimising the laser treatment is crucial. This can be achieved either by selecting cutting parameters that create grooves without damaging the resin or by adjusting the line spacing to balance surface modification and substrate integrity.

Acknowledgements

The authors would like to thank CAPES (scientific initiation scholarship), FAPEMIG (APQ-04336-23 and APQ-01007-25) and CNPq (PQ 305553/2023-2 and 405506/2023-6) for the financial support provided.

Author contributions

LFS: Data curation, Methodology, Formal analysis, investigation, Writing – original draft. TF: Data curation, Formal analysis, Investigation, Writing – original draft, Writing – review & editing. AJBC: Data curation, Writing – review & editing. THP: Conceptualization, Funding acquisition, Resources, Supervision, Writing – review & editing. MG: Conceptualization, Supervision, Writing – review & editing. PC: Conceptualization, Supervision, Writing – review & editing. FS: Conceptualization, Supervision, Writing – review & editing.

Declaration of Competing Interest

The authors declare no conflicts of interest.

Data availability statement

Data supporting these findings are available within the article or upon request.

References

[1] Cascino, A., Meli, E. & Rindi, A. A strategy for lightweight designing of a railway vehicle car body including composite material and dynamic structural optimization. Rail. Eng. Science 31,340–350 (2023). https://doi-org.ez32.periodicos.capes.gov.br/10.1007/s40534-023-00312-6)

[2] Kumar CS, Arumugam V, Kennedy JJ, Karthikeyan R, Jac Fredo AR. Experimental investigation on the effect of glass fiber orientation on impact damage resistance under cyclic indentation loading using AE monitoring. Nondestructive Testing and Evaluation. 2020;35(4):408–426. doi:10.1080/10589759.2019.1684491

[3] Gualberto, Hiasmim Rohem; do Carmo Amorim, Felipe; Costa, Hector Reynaldo Meneses. A review of the relationship between design factors and environmental agents regarding adhesive bonded joints. Journal of the Brazilian Society of Mechanical Sciences and Engineering, v. 43, n. 8, p. 389, 2021. (https://doi.org/10.1007/s40430-021-03105-2)

[4] Gualberto H, Wang L, et al. Progress in adhesive joint technologies. Journal of Materials Engineering. 2021;37:421–433; 2023;39:501–515.

[5] Karthikeyan N, Jesuarockiam N. Progress in adhesive-bonded composite joints: A comprehensive review. Journal of Reinforced Plastics and Composites. 2024. doi:10.1177/07316844241248236

[6] Wang D, et al. Increasing strength and fracture toughness of carbon fibre-reinforced plastic adhesively bonded joints by combining peel-ply and oxygen plasma treatments. Applied Surface Science. 2023;612:155768. https://doi.org/10.1016/j.apsusc.2022.155768

[7] Hennemann OD, Brockmann W. Surface morphology and its influence on adhesion. Journal of Adhesion. 1981;12(4):297–315. doi:10.1080/00218468108071208

[8] Liu J, et al. Review of the surface treatment process for the adhesive matrix of composite materials. International Journal of Adhesion and Adhesives. 2023;126:103446. doi.org/10.1016/j.ijadhadh.2023.103446

[9] Musiari F, Moroni F, Lutey AHA. Enhanced mechanical interlocking of adhesive-bonded joints via tailored serrated patterns manufactured with laser ablation. The Journal of Adhesion. 2023:1–35. doi:10.1080/00218464.2023.2285431

[10] Mottaghian F, Taheri F. Effects of surface treatment on the strength of double-strap adhesively bonded joints mating 3D-fiber metal laminates. Materials Letters. 2022;324:132698. doi:10.1016/j.matlet.2022.132698

[11] Liu Z, Li S, Yu Y. CFRTP single-lap adhesive bonding and its mechanical performance enhanced by laser surface treatment: Finite element simulation and experimental validation. Optics & Laser Technology. 2025;181:111765. https://doi.org/10.1016/j.optlastec.2024.111765

[12] Li H, et al. Influence of high pulse fluence infrared laser surface pretreatment parameters on the mechanical properties of CFRP/aluminium alloy adhesive joints. The Journal of Adhesion. 2023;99(4):584–605. https://doi.org/10.1080/00218464.2022.2027242

[13] İplikçi H, et al. Effects of nanosecond laser ablation parameters on surface modification of carbon fiber reinforced polymer composites. Journal of Composite Materials. 2023;57(18):2843–2855. https://doi.org/10.1177/00219983231178892

[14] Liu Z, et al. Laser-induced surface reconstruction to enhance interfacial bonding reliability of CFRP/titanium hybrid joints. Journal of Materials Research and Technology. 2024;32:3523–3536. https://doi.org/10.1016/j.jmrt.2024.08.099

[15] Schanz J, et al. Laser-based surface treatment of CFRP and aluminum for adhesively bonded hybrid joints. In: Laser-based Micro-and Nanoprocessing XIV. SPIE; 2020. p. 262–272.

[16] Leone C, Genna S. Effects of surface laser treatment on direct co-bonding strength of CFRP laminates. Composite Structures. 2018;194:240–251.

[17] Bora MO, et al. Comparison of novel surface treatments of Al 2024 alloy for Al/CFRP adhesive bonded joints. International Journal of Adhesion and Adhesives. 2020;103:102721.

[18] Wu Y, et al. Effect of laser ablation surface treatment on performance of adhesive-bonded aluminum alloys. Surface and Coatings Technology. 2016;304:340–347.

[19] Li H, et al. Effect of laser-generated microgroove geometric parameters on the shear strength of CFRP-aluminum alloy adhesive joints. The Journal of Adhesion. 2023;99(10):1744–1767. doi:10.1080/00218464.2022.2158731

[20] Abedinzadeh Andarabi A, Shelesh-Nezhad K, Chakherlou TN. The effect of laser surface structuring patterns on the interfacial resistance of aluminum joints bonded with epoxy adhesive. International Journal of Adhesion and Adhesives. 2022;114:103101. doi:10.1016/j.ijadhadh.2022.103101

[21] Zou X, et al. Laser surface treatment to enhance the adhesive bonding between steel and CFRP: Effect of laser spot overlapping and pulse fluence. Optics & Laser Technology. 2023;159:109002. doi:10.1016/j.optlastec.2022.109002

[22] Luo J, et al. Surface treatments for enhancing the bonding strength of aluminum alloy joints. Materials. 2023;16(16):5674. doi:10.3390/ma16165674

[23] Badami A, et al. Surface roughness influence on the behaviour of biocomposite adhesive joints. International Journal of Mechanical Sciences. 2024;283:109624. doi:10.1016/j.ijmecsci.2024.109624

[24] Wang F, et al. Influence of the different surface treatments on fracture property of CFRP adhesive joint. Journal of Adhesion Science and Technology. 2022;37(6):961–975. doi:10.1080/01694243.2022.2060785

[25] Naat N, et al. Effect of surface texture on the mechanical performance of bonded joints: a review. The Journal of Adhesion. 2021;99(2):166–258. doi:10.1080/00218464.2021.2008370

[26] Maggiore S, et al. A review of structural adhesive joints in hybrid joining processes. Polymers. 2021;13(22):3961.

[27] Xiang S, et al. Experimental and numerical investigation on failure behavior of hybrid bonded/bolted GFRP single-lap joints under static shear loading. Engineering Failure Analysis. 2024;158:107969. doi:10.1016/j.engfailanal.2024.107969

[28] Sharma A, et al. Combined computational-experimental investigation of residual stresses and pre-cracking in mode I behaviour of thick adhesively bonded GFRP composite joints. Composite Structures. 2025;351:118549. https://doi.org/10.1016/j.compstruct.2024.118549

[29] Fan J, Vassilopoulos AP, Michaud V. Mode I fracture of thick adhesively bonded GFRP composite joints for wind turbine rotor blades. Composite Structures. 2024;327:117705. https://doi.org/10.1016/j.compstruct.2023.117705

[30] ASTM D5868-01(2014). Standard Test Method for Lap Shear Adhesion for Fiber Reinforced Plastic (FRP) Bonding. ASTM International, West Conshohocken, PA, 2014. doi:10.1520/D5868-01R14

[31] ASTM D5377. Standard Practice for Classifying Failure Modes in Fiber-Reinforced-Plastic (FRP) Joints. ASTM International, West Conshohocken, PA, 2014.

[32] Rangaswamy H, et al. Experimental analysis and prediction of strength of adhesive-bonded single-lap composite joints: Taguchi and artificial neural network approaches. SN Applied Sciences. 2020;2:1–15.



https://dspace.org/

Plain weave glass-fibre composite joints With Co2 Laser ablation architected treatments

Soares, Luiza; Ferreira, Thayane; Campuzano, Alberto; Grasso, Marzio; Camanho, Pedro ...

2026-01
Sage
https://doi.org/10.1177/14644207251382566
Soares L, Ferreira T, Campuzano A, et al., (2025) Plain weave glass-fibre composite joints With Co2 Laser ablation architected treatments. Proceedings of the Institution of Mechanical Engineers, Part L: Journal of Materials: Design and Applications, Available online 31 October 2025, Article number 14644207251382566

Downloaded from a DSpace repository. https://dspace.org/